

Resistance Noise Near to Electrical Breakdown: Steady State of Random Networks as a Function of the Bias

C. Pennetta

*INFN - National Nanotechnology Laboratory, and Dipartimento di Ingegneria dell'Innovazione,
Università di Lecce, Italy, Via Arnesano, I-73100, Lecce, Italy, **

A short review is presented of a recently developed computational approach which allows the study of the resistance noise over the full range of bias values, from the linear regime up to electrical breakdown. Resistance noise is described in terms of two competing processes in a random resistor network. The two processes are thermally activated and driven by an electrical bias. In the linear regime, a scaling relation has been found between the relative variance of resistance fluctuations and the average resistance. The value of the critical exponent is significantly higher than that associated with $1/f$ noise. In the nonlinear regime, occurring when the bias overcomes the threshold value, the relative variance of resistance fluctuations scales with the bias. Two regions can be identified in this regime: a moderate bias region and a pre-breakdown one. In the first region, the scaling exponent has been found independent of the values of the model parameters and of the bias conditions. A strong nonlinearity emerges in the pre-breakdown region which is also characterized by non-Gaussian noise. The results compare well with measurements of electrical breakdown in composites and with electromigration experiments in metallic lines.

Noise; breakdown; percolation; random networks.

I. INTRODUCTION

A large interest exists in the recent literature concerning the electrical and mechanical stability of different physical systems¹⁻²⁵. In fact, from a technological point of view, the increasing level of miniaturization of electronic devices enhances the importance of degradation and failure processes^{4, 20, 25-31}. On the other hand, from a theoretical point of view, the study of the response of disordered systems to high external stresses, implied in the study of breakdown and fracture processes, is of great help to understand the properties of these systems and, more generally, to develop the knowledge of nonequilibrium systems^{1-12, 32-35}. It is well known that the application of a finite stress (electrical or mechanical) to a disordered material generally gives a nonlinear response, which ultimately leads to an irreversible breakdown (catastrophic behavior) in the high stress limit¹⁻⁴. Such breakdown phenomena have been successfully studied by using percolation theories^{1-3, 6-9, 13-25, 30, 36-42}. In particular, by focusing on electrical breakdown, a large attention has been devoted to the determination, by both theory^{1-3, 6, 7, 20, 36-42} and experiments^{1-3, 13-18} of the critical exponents describing the resistance and the variance of resistance fluctuations in terms of the conducting particle (or defect) concentration^{36, 37}. In fact, it is well known that the study of the resistance fluctua-

tions is a fundamental tool to extract information about the system stability^{1-4, 27-29, 39-48}. In spite of the wide literature on the subject few attempts have been made so far^{21, 22} to describe the behavior of a disordered medium over the full range of the applied stress, i.e. by studying the response of the system to an external bias when the bias strength covers the full range of linear and nonlinear regimes. On the other hand, important information are expected from this kind of study, like: precursor phenomena, role of the disorder, existence of scaling laws, predictability of breakdown, etc.

Recently, a new approach has been proposed to investigate the resistance noise in thin films over the full range of bias values, from the linear regime up to electrical breakdown⁴⁹⁻⁵¹. In this paper, I will present a brief review of this approach. The model consists of describing the resistance noise in a conducting film in terms of two competing processes taking place in a random resistor network (RRN)⁴⁹⁻⁵¹. The two processes are driven by the joint effect of the electrical bias and of the heat exchange with a thermal bath. The breaking of a single resistor of the network is taken as a simple and general manner to account for different microscopic mechanisms which are responsible for the degradation of the electrical properties of a small region of the film. This defect generation process is taken to occur in competition with

*Corresponding authors e-mail: cecilia.pennetta@unile.it

an opposite process, named defect recovery, which mimics the healing mechanisms. Electromigration of metallic lines^{4,26} instability of the electrical properties of composites or semicontinuous metal films^{2,3, 13-19, 22,23} or soft dielectric breakdown of ultra-thin oxides^{4,29}, are examples of phenomena that can be successfully described by this approach^{25,31,49-51}. In the case of electromigration phenomena, for example, the defect generation corresponds to the formation of voids induced by the electronic wind, while the defect recovery is related to the void healing due to mechanical stress and thermal gradients inside a metallic film^{4,26}. In the case of composites, the electrical instability arises from the opening of new conductive channels as a consequence of thermally activated hopping processes^{2,22}. On the other hand, the same processes can also lead to a suppression of already existing channels. In the case of soft dielectric breakdown of ultra-thin oxides it is instead the competition between electron trapping and detrapping which plays a key role on leakage currents^{4,29,30}.

All these phenomena and many others^{1-3, 28,52} can be modeled in terms of competition between two opposed processes taking place in a RRN. Monte Carlo simulations show that, depending on the bias strength, an irreversible failure or a stationary state of the RRN can be achieved. By focusing on the steady-state, the behavior of the average network resistance and the properties of the resistance fluctuations are analyzed as a function of the bias. At low bias, an effective defect generation probability can be defined controlling the network behavior⁴⁹. In this Ohmic regime, a scaling relation has been found between the relative variance of resistance fluctuations and the average network resistance⁴⁹. The properties of the nonlinear regime, occurring when the bias overcomes a threshold value, are studied for different values of the model parameters and for different bias conditions (constant voltage or constant current)^{50,51}. Scaling relations are found relating the average resistance and the resistance noise with the external bias. In particular, a strong nonlinearity emerges in the pre-breakdown region which is also characterized by a non-Gaussian noise. The results compare well with measurements of electrical breakdown in composites^{2,22,19} and in semicontinuous metal films¹⁶ and with electromigration experiments in metallic lines^{26,25}.

II. THEORY

The RRN consists of a two-dimensional square-lattice network made of N_{tot} resistors of resistance r_n ³⁶. Different geometries can be studied; here we consider the simplest one which is the square $N \times N$, where N determines the linear size of the network. In practical applications the value of N can be related to the ratio between the size of the film and that of the characteristic grain. The RRN exchanges heat with a thermal bath at temperature T_0

(substrate temperature). A current I , kept constant, is applied to the network through electrical contacts at the left and right hand sides. Alternatively, constant voltage conditions can be considered. The current flowing in the n -th resistor of the network is denoted by i_n . The resistances are taken linearly dependent on temperature through a temperature coefficient of resistance, α :

$$r_n(T_n) = r_0[1 + \alpha(T_n - T_0)] \quad (1)$$

The local temperature T_n is calculated by adopting the biased percolation model^{54,24} as:

$$T_n = T_0 + A \left[r_n i_n^2 + \frac{B}{N_{neig}} \sum_{l=1}^{N_{neig}} (r_l i_l^2 - r_n i_n^2) \right] \quad (2)$$

where N_{neig} is the number of first neighbors around the n th resistor. The parameter A , measured in (K/W), describes the heat coupling of each resistor with the thermal bath and it determines the importance of Joule heating effects. The parameter B is taken to be equal to 3/4 to provide a uniform heating in the perfect network configuration. It must be noticed that Eq. (2) implies an instantaneous thermalization of each resistor at the value T_n , thus, by adopting Eq. (2), we are neglecting for simplicity time dependent effects which are discussed in Ref.⁸.

Here, the initial state of the network is chosen coinciding with the perfect network ($r_n \equiv r_0$) of resistance R_0 . Nevertheless, a disordered initial configuration can easily be introduced in the present approach to analyze the role of the initial disorder on the RRN response. We assume that two competing processes act to determine the RRN evolution. The first process consists of generating fully insulating defects (resistors with very high resistance, i.e. broken resistors) with probability²⁰ $W_{D,n} = \exp(-E_D/K_B T_n)$, where E_D is a characteristic activation energy and K_B the Boltzmann constant. The second process consists of recovering the insulating defects with probability $W_{R,n} = \exp(-E_R/K_B T_n)$, where E_R is an activation energy characteristic of this second process^{25,49}. Thus, the first process consists in a percolation of broken resistors within a network of active resistors. This percolative process is contrasted by a recovery process. This second process can also be seen as a percolation of active resistors within an insulating network. For $A \neq 0$, Eq. (2) implies that both the processes (defect generation and defect recovery) are correlated processes. Indeed, the probability of breaking (recovering) a resistor is higher in the so called ‘‘hot spots’’ of the RRN³⁶. On the other hand, for $A = 0$ Eq. (2) yields $T_n \equiv T_0$, which corresponds to the competition of two random processes^{36,49}. The same is true for vanishing small bias values, when Joule heating effects are negligible.

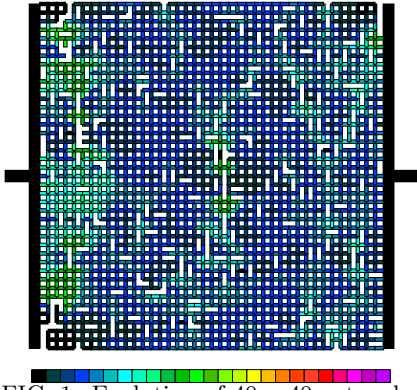


FIG. 1. Evolution of 40×40 network obtained for a value of the external current $I = 1.2$ (A). The different colors, from black to violet, correspond to increasing values of r_n from 1 to 15 (Ω). The pattern shown corresponds to the iteration step $t = 800$.

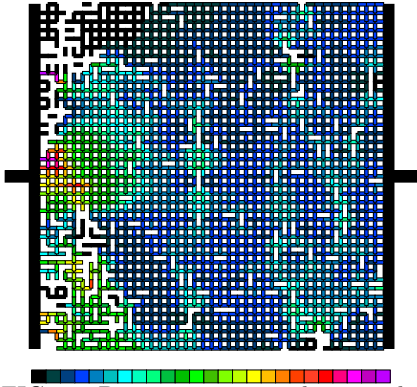


FIG. 2. Pattern corresponding to the same evolution of Fig. 1 and to the iteration step $t = 805$.

The sequence, defect-creation and defect-recovery, is then iterated. Depending on the material parameters (E_D , E_R , A , α , r_0 , N) and on the external conditions (specified by the kind of applied bias and by the bath temperature) a steady state or an irreversible breakdown characterized by a critical fraction of defects p_c (percolation threshold) are reached. In the first case, the network resistance fluctuates around an average value $\langle R \rangle$. In the second case, R diverges due to the existence of at least one continuous path of defects between the upper and lower sides of the network³⁶. We note that in the limit of a vanishing bias (two random processes) and infinite lattices ($N \rightarrow \infty$), the expression: $E_R < E_D + K_B T_0 \ln[1 + \exp(-E_D/K_B T_0)]$ provides a sufficient condition for the existence of a steady state⁴⁹. In the general case of biased processes, no analytical expressions are available for the steady state condition and thus it is necessary to rely on numerical simulations only.

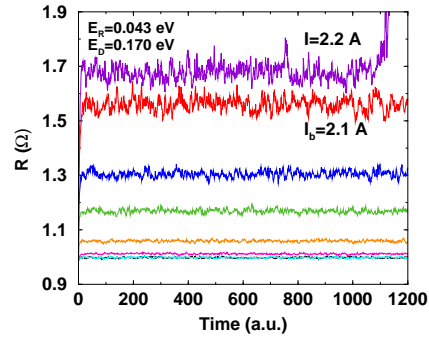


FIG. 3. Resistance evolutions for increasing bias values. Going from bottom to top, the curves are obtained for $I = 0.01, 0.1, 0.5, 1.0, 1.5, 1.8, 2.1$ (A) and they correspond to RRN steady states. Precisely, the highest curve shows an unsteady evolution of the resistance obtained for $I = 2.2$ (A), the curve just below corresponds to the breakdown current $I_b = 2.1$.

The evolution of the RRN is obtained by MC simulations carried out according to the following procedure. (i) Starting from the perfect lattice with given local currents, the local temperatures T_n are calculated according to Eq. (2); (ii) the defects are generated with probability W_D and the resistances of the unbroken resistors are changed as specified by Eq. (1); (iii) the currents i_n are calculated by solving Kirchhoff's loop equations by the Gauss elimination method and the local temperatures are updated; (iv) the defects are recovered with probability W_R and the temperature dependence of unbroken resistors is again accounted for; (v) R , i_n and T_n are finally calculated and the procedure is iterated from (ii) until one of the two following possibilities is achieved. In the first, the percolation threshold is reached. In the second, the RRN attains a steady state; in this case the iteration runs long enough to allow a fluctuation analysis to be carried out. Each iteration step can be associated with an elementary time step on an appropriate time scale (to be calibrated with experiments). In this manner it is possible to represent the simulated resistance evolution over either a time or a frequency domain according to convenience. Except when differently specified, the simulations are performed by taking the following values for the parameters, which are chosen as reasonable values: $N = 75$, r_0 ranges from $1 \div 10$ (Ω), $\alpha = 10^{-3}$ (K^{-1}), $A = 5 \times 10^5$ (K/W), $E_D = 0.170$ (eV), E_R in the range $0.026 \div 0.155$ (eV) and $T_0 = 300$ (K). The values of the external bias range from $0.001 \leq I \leq 3.0$ (A) under constant current conditions, and from $0.001 \leq V \leq 3.5$ (V) under constant voltage conditions. Further details about numerical simulations can be found in Refs.^{24,49-51}.

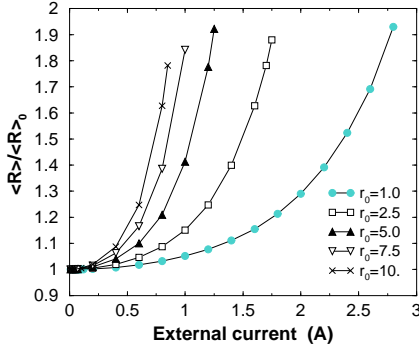


FIG. 4. Average resistance versus the external current. The resistance is normalized to the linear regime value. The different curves are obtained for $E_D = 0.17$ (eV) and $E_R = 0.026$ (eV), while r_0 ranges from 1 to 10 (Ω).

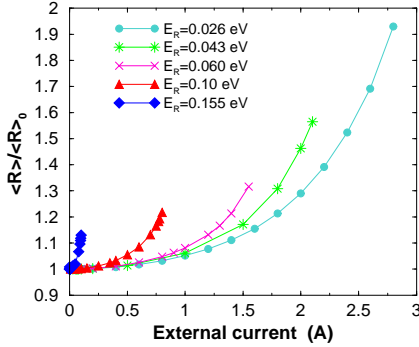


FIG. 5. Average resistance versus the external current. The resistance is normalized to the linear regime value. The different curves are obtained for $E_D = 0.17$ (eV) and $r_0 = 1$ (Ω), while E_R ranges from 0.026 to 0.155 (eV).

III. RESULTS

Figures 1 and 2 display the evolution of a 40×40 network, made of resistors with $r_0 = 1.0$ (Ω), characterized by a value of $E_R = 0.043$ (eV) and subjected to a bias current $I = 1.2$ (A). For this choice of the parameters, the network becomes unstable for currents greater than $I_b = 1.1$ (A). Therefore, in the case considered, the network evolves towards the electrical breakdown which is reached after 809 iteration steps. Precisely, Fig. 1 shows the formation of filamented clusters of defects (missing resistors) characteristic of biased percolation^{24,52}. Figure 2 reports the pattern very near to the final breakdown. The incipient cluster of defects, perpendicular to the direction of the applied current is well evident, together with the formation of hot spots. This kind of damage pattern perfectly agrees with the pattern observed in metallic lines failed as a consequence of electromigration^{4,26}.

Typical resistance evolutions of a 75×75 RRN, with the same parameters used for Figs. 1 and 2, are reported in Fig. 3 for different values of the bias current. The first six curves from the bottom correspond to steady

states of the RRN, the upper curve to an evolution toward electrical breakdown. In particular, it must be noticed that the first two curves (black and cyan), obtained for $I = 0.01$ (A) and $I = 0.1$ (A), are practically overlapping. By contrast, all the other steady state curves fluctuate around significantly different average values with increasing fluctuation amplitudes. Thus, the figure well illustrates a general feature of the model: the ability of describing both the linear and the nonlinear regimes up to the breakdown.

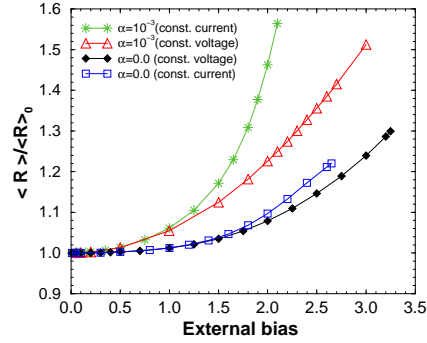


FIG. 6. Normalized average resistance versus the external bias: constant current for the green and blue curves, constant voltage for the red and black ones. Precisely, the green and red curves are obtained for $\alpha = 10^{-3}$ (K^{-1}) while the blue and black for $\alpha = 0$. The other parameters are specified in the text. The bias values are in A and in V units under constant current and constant voltage, respectively.

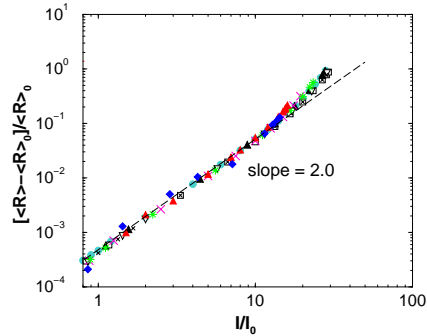


FIG. 7. Log-log plot of the relative variation of the average resistance versus the normalized current. Only the nonlinear regime is shown. The data correspond to different values of E_R and to different values of r_0 and they are the same shown in Figs. 4 and 5. The dashed line fits the data in the moderate bias region.

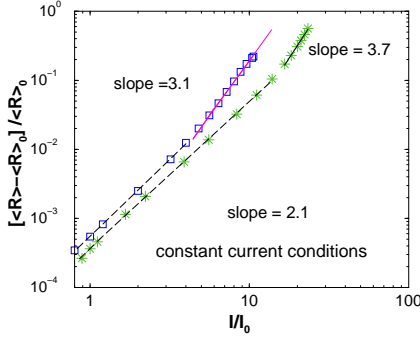


FIG. 8. Log-log plot of the relative variation of the average resistance versus the normalized current. Only the nonlinear regime is shown. The data indicated with green stars are obtained for $\alpha = 10^{-3}$ (K^{-1}), while the data indicated with blue squares for $\alpha = 0$. The dashed black lines fit the data with a power-law of exponent 2.1, the magenta line with a power-law of exponent 3.1 and the black solid line corresponds to an exponent 3.7.

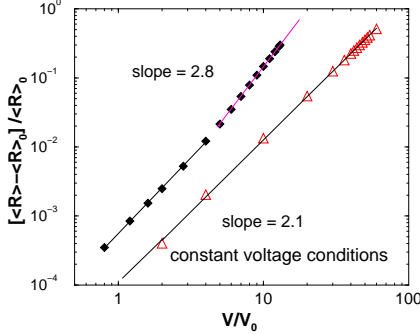


FIG. 9. Log-log plot of the relative variation of the average resistance versus the normalized voltage. The data indicated with red triangles are obtained for $\alpha = 10^{-3}$ (K^{-1}), while the data indicated with black diamonds for $\alpha = 0$. The black lines fit the data with a power-law of exponent 2.1 while the magenta line with a power-law of exponent 2.8.

Figure 4 shows the average values of the RRN resistance as a function of the bias current. Each value is calculated by considering the time average on a single steady-state realization and then averaging over 20 independent realizations. Further details can be found in Ref.⁵¹. The different curves correspond to different values of r_0 , as specified in the figure, and to a common value of $E_R = 0.026$ (eV). At the lowest biases the average resistance is independent of the bias values and it takes a value $\langle R \rangle_0$, which represents the linear response of the network (Ohmic regime)⁴⁹. For this reason in Fig. 4 the average resistance has been normalized to $\langle R \rangle_0$. At increasing biases, when the current overcomes a certain value, I_0 , the average resistance starts to become dependent on the bias. Thus, I_0 sets the current scale value for the onset of nonlinearity. The average resistance increases with bias up to a value $\langle R \rangle_b$, which corresponds to a threshold current I_b . Above this threshold current the RRN undergoes an irreversible breakdown.

Details about the criteria used for the determinations of I_0 and I_b can be found in Ref.⁵¹. It must be noticed that by increasing the initial RRN resistance, both I_b and I_0 decrease but the ratios I_b/I_0 and $\langle R \rangle_b / \langle R \rangle_0$ are found to be independent of the initial resistance value⁵⁰. Moreover, these ratios are found independent of the network sizes⁵³. Both these behaviors agree with electrical breakdown measurements performed in composites²² and in semicontinuous metal films¹⁶.

Figure 5 reports the normalized average resistance as a function of the bias current for different values of the recovery activation energy, specified in the figure. All the curves are now obtained by taking $r_0 = 1$ (Ω). In this case, not only I_b and I_0 decrease with E_R but also the ratios I_b/I_0 and $\langle R \rangle_b / \langle R \rangle_0$ diminish⁵⁰. Thus, in contrast to what happens for the effect of the initial resistance, the decreasing robustness of the system is associated with a reduction of the extent of the nonlinear region. It must be underlined that if the value of E_R is sufficiently different from its maximum value $E_{R,MAX}$ (determined by the stability condition in the vanishing bias limit, discussed in Sec. 2) the threshold current I_b is associated with a first order transition. In fact, the “last” stable state of the RRN, corresponding to I_b , is characterized by an average defect fraction $\langle p \rangle_b$ which is smaller than p_c . Therefore, the correlation length and the correlation time remain finite at the threshold⁵³, denoting a non critical behavior. It must be noticed that the prediction of a first order transition is confirmed by experiments^{2,22}.

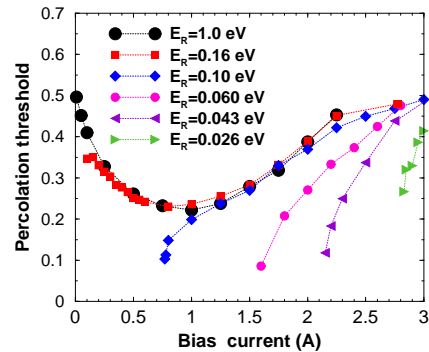


FIG. 10. Percolation threshold versus the external current for different values of the recovery energy E_R which ranges from 0.026 (eV) to 1.0 (eV).

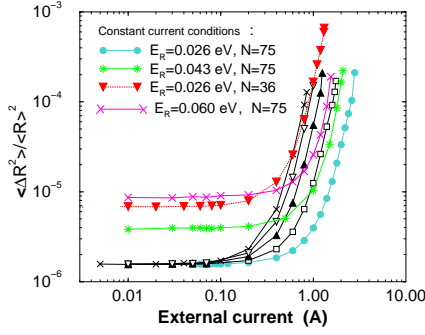


FIG. 11. Relative variance of resistance fluctuations versus the external current. Magenta, green and cyan curves correspond to decreasing values of E_R . The black curves are obtained for the same value of E_R used for the cyan curve and they differ for the value of r_0 . Precisely, cyan circles $r_0 = 1.0$, open square $r_0 = 2.5$, black triangles $r_0 = 5.0$, open triangles $r_0 = 7.5$, crosses $r_0 = 10.0$. The values of r_0 are expressed in Ω . The red curve with down triangles is obtained for the same parameters of the cyan curve but for a smaller network, of size $N = 36$.

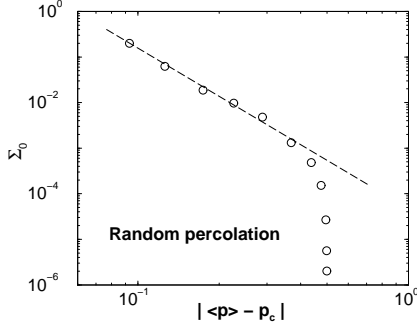


FIG. 12. Relative variance of resistance fluctuations versus $| \langle p \rangle - p_c |$ in the linear regime. This regime corresponds to the competition of two random processes.

The effect of the temperature coefficient of the resistance, α , is shown in Fig. 6, where we have also reported the behaviors of the average resistance calculated under constant current and under constant voltage conditions. The simulations are performed by taking $r_0 = 1$ and $E_R = 0.043$ (eV). Similarly to the constant current case, also under constant voltage two threshold voltage values exist: V_0 and V_b , corresponding to the nonlinearity onset and to the electrical breakdown, respectively. The ratio V_b/V_0 is found to be significantly higher than the ratio I_b/I_0 ⁵¹. This fact reflects the greatest stability of the system when biased under constant voltage than under constant current. This property is further emphasized by the fact that the increase of the resistance in the pre-breakdown region exhibits a lower slope under constant voltage than under constant current conditions, as discussed below. It must be noticed that in spite of the significant difference of the ratios V_b/V_0 and I_b/I_0 , the ratio $\langle R \rangle_b / \langle R \rangle_0$ remains practically the same under the different bias conditions⁵¹, in agreement with experiments²².

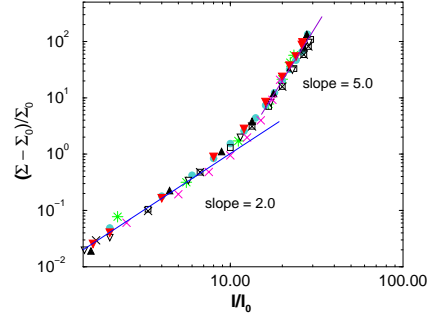


FIG. 13. Log-log plot of the relative variation of Σ versus I/I_0 . The data shown are obtained for different values of E_R , r_0 and N and they are the same of Fig. 11. The black line fits the different sets of data in the moderate bias region with a power-law of exponent 2.0, while the blue line of slope 5.0 in the high bias region is only for a guide to the eyes.

To analyze the dependence on the bias of the average resistance and to investigate the existence of scaling relations and their universality³³, Fig. 7 reports on a log-log plot the relative variation of the average resistance, $\Delta \langle R \rangle / \langle R \rangle_0 \equiv (\langle R \rangle - \langle R \rangle_0) / \langle R \rangle_0$, as a function of I/I_0 for different values of r_0 and E_R . The data are the same of Figs. 4 and 5. The figure shows that all the curves collapse onto a single one and that the relative variation of $\langle R \rangle$ scales with the ratio I/I_0 as⁵⁰:

$$\frac{\langle R \rangle}{\langle R \rangle_0} = g(I/I_0), \quad g(I/I_0) \simeq 1 + a(I/I_0)^\theta \quad (3)$$

with the exponent $\theta = 2.1 \pm 0.1$ and a a dimensionless coefficient. However, it must be noticed that a superquadratic behavior of $\langle R \rangle$ emerges in the pre-breakdown region, where the relative variation of $\langle R \rangle$ is characterized by a power law $(I/I_0)^{\theta_I}$ with an exponent $\theta_I = 3.7 \pm 0.3$ ⁵¹. Furthermore, this superquadratic behavior emerges only for RRN sufficiently robust. In fact, at increasing the recovery activation energy E_R , the ratio I_b/I_0 becomes smaller, i.e. the stability region is reduced and the dependence on the current of the average resistance can remain quadratic over the entire region.

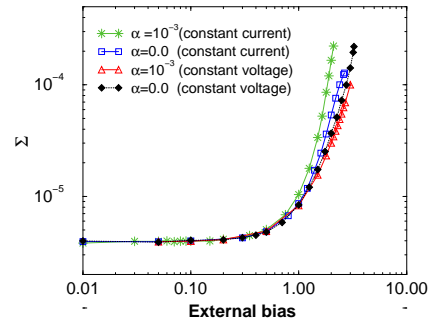


FIG. 14. Relative variance of resistance fluctuations versus the external bias: constant current for the green and blue curves, constant voltage for the red and black ones. Precisely, the green and red curves are obtained for $\alpha = 10^{-3} \text{ (K}^{-1}\text{)}$ while the blue and black for $\alpha = 0$. The other parameters are specified in the text. The bias values are in A and in V units under constant current and constant voltage, respectively

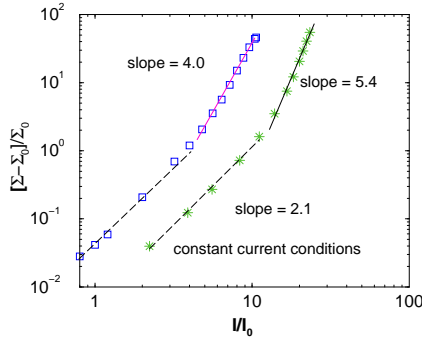


FIG. 15. Log-log plot of the relative variance of resistance fluctuations versus the normalized current. The data indicated with green stars are obtained for $\alpha = 10^{-3} \text{ (K}^{-1}\text{)}$, while the data indicated with blue squares for $\alpha = 0$. The black dashed lines fit the data with a power-law of exponent 2.1, the black solid line with a power-law of exponent 5.4, while the magenta solid line corresponds to an exponent 4.0.

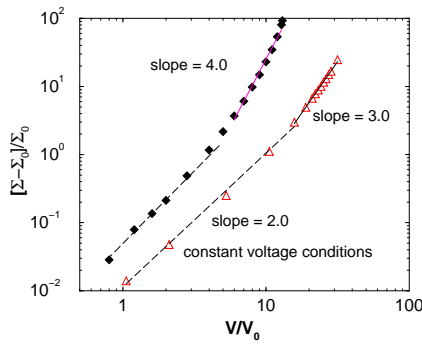


FIG. 16. Log-log plot of the relative variance of resistance fluctuations versus the normalized voltage. The data indicated with red triangles are obtained for $\alpha = 10^{-3} \text{ (K}^{-1}\text{)}$, while the data indicated with black diamonds for $\alpha = 0$. The black dashed lines fit the data with a power-law of exponent 2.0, the black solid line with a power-law of exponent 3.0, while the magenta solid line corresponds to an exponent 4.0.

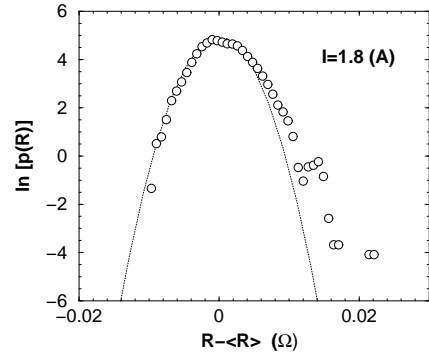


FIG. 17. Distribution function of the resistance fluctuations for an applied current of $I = 1.8 \text{ (A)}$, the other parameters are specified in the text. The scale is a linear-log, therefore the dashed curve corresponds to a Gaussian distribution.

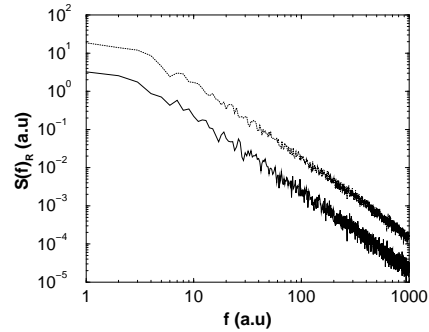


FIG. 18. Power spectral density of resistance fluctuations under constant current conditions. The solid curve is obtained for $I = 1.5 \text{ (A)}$, the dotted one for $I = 1.8 \text{ (A)}$.

In the log-log plot reported in Fig. 8 we compare the relative variations of the resistance versus the ratio I/I_0 calculated for two different values of the temperature coefficient: $\alpha = 10^{-3} \text{ (K}^{-1}\text{)}$ and $\alpha = 0$ (the data are the same as those shown in Fig. 6 with stars and open squares respectively). We can see that the two sets of data do not collapse onto the same curve, i.e. they do not belong to the same universality class. Moreover, the effect of a nonzero value of α is to significantly enhance the superquadratic dependence of the resistance on the bias under constant current conditions. By contrast, the opposite is true under constant voltage conditions, as shown in Fig. 9, where the data obtained for $\alpha = 10^{-3} \text{ (K}^{-1}\text{)}$ are again compared with those obtained for $\alpha = 0$ (same data shown in Fig. 6 with triangles and full squares, respectively). In fact, in this case, the effect of α is to depress the superquadratic behavior. Remarkably, under constant voltage conditions, the average resistance scales quadratically with the applied voltage over the whole region of bias values up to breakdown, as⁵¹:

$$\frac{\langle R \rangle_V}{\langle R \rangle_0} = 1 + a' \left(\frac{V}{V_0} \right)^\theta \quad (4)$$

where a' is a dimensionless coefficient and the value of θ is the same of that in Eq. (3).

The quadratic dependence on the bias in the moderate bias region, common to all the data shown in Figs. 7, 8 and 9, must be considered a general feature of the model, in agreements with experiments²² and can be explained as follows. It is well known³⁶ that the resistance of sufficiently large RRNs subjected to random percolation is related to the fraction of broken resistors by the scaling relation:

$$R \sim |p - p_c|^{-\mu} \quad (5)$$

where $p_c \equiv p_{c0} = 0.5$ for a square lattice and μ takes a universal value, known from very accurate calculations: $\mu = 1.303$ for two-dimensional RRNs³⁶. This scaling relation should hold also for steady states of RRNs resulting from the superposition of two opposite random processes. In this case, Eq. (5) relates the average network resistance $\langle R \rangle$ with the average fraction of defects $\langle p \rangle$. Numerical simulations reported in Ref.⁴⁹ confirm this statement. On the other hand, when a single biased percolation is present p_c becomes a function of the bias strength^{55,54} (see black circles in Fig. 10), moreover the value of μ is no more universal and it depends on the biasing conditions^{54,24}. When two competing biased processes are present, leading to steady states of the RRN, the use of Eq. (5) becomes quite problematic. In fact, in this case p_c depends also on the recovery activation energy, as shown in Fig. 10. In this figure the black circles represent p_c versus the bias when $E_R \gg E_D$ so that no recovery of defects occurs. In this case the RRN is unstable for any value of the applied current and, at vanishing bias, p_c takes the random percolation value p_{c0} . At increasing bias, the correlated growth of defects along filamented clusters reduces p_c . At still higher values of the bias, a multi-channel filamentation emerges⁵⁵ which makes p_c an increasing function of I . When $E_R < E_D$ a stability region appears for $I < I_b$, whose extent increases at decreasing E_R , as shown in Fig. 5. Therefore, the corresponding curves in Fig. 10 start at progressively higher values of I . In spite of these complications, at moderate bias and when $\langle p \rangle \ll p_c$, by truncating Eq. (5) to the first order in $\langle p \rangle / p_c$, we can write: $\Delta \langle R \rangle \approx C(\mu_0, p_{c0}) \Delta \langle p \rangle$. Furthermore, in the spirit of a mean-field theory, it is possible to see⁵¹ that the relative variation of the average defect fraction: $\Delta \langle p \rangle / \langle p \rangle_0 \propto (I/I_0)^2$. Thus, also $\Delta \langle R \rangle \propto (I/I_0)^2$. At high bias, terms of order higher than the first in the expansion of $\langle R \rangle$ in terms of $\langle p \rangle / p_c$ and the dependence on the bias of p_c become important. Furthermore, $\Delta \langle p \rangle$ is no more a quadratic function of the bias⁵¹. Therefore, the average resistance acquires the superquadratic behavior shown in Figs. 7, 8 and 9. On the basis of the previous results and of the above discussion, the behavior of the average resistance in the moderate bias region is expected to be a universal feature. Of course a final validation of this statement would require a study of the effect of the network topology (non square lattices, etc.) and of the boundary conditions.

The relative variance of resistance fluctuations, $\Sigma \equiv \langle \Delta R^2 \rangle / \langle R \rangle^2$, is reported in Fig. 11 as a function of I and for different r_0 and E_R values. The data correspond to the same simulations shown in Figs. 4 and 5 and they are obtained by using the same procedure of time averaging over a single simulation and then ensemble averaging over 20 realizations. Only the three lowest values of E_R used in Fig. 5 have been reported in Fig. 11 and with the same symbols. In addition, the red curve with down triangles shows the relative variance Σ obtained for a network of size 36×36 . All the other parameters are the same as those ones used for the curve with cyan circles ($E_R = 0.026$ eV and $r_0 = 1.0$). At low bias, the relative variance of resistance fluctuations is found to achieve a constant value Σ_0 which represents an intrinsic property of the system. On the other hand, a strong increase of Σ characterizes the nonlinear regime occurring for $I > I_0$.

By focusing on Σ_0 , we can see in Fig. 11 that this quantity is independent of r_0 but strongly dependent on the recovery activation energy E_R . In fact Σ_0 , corresponding to the vanishing bias limit, arises from the competition of two random processes. The study of the resistance noise in RRNs subjected to two random processes, has been performed in Ref.⁴⁹ and it pointed out the following results. Σ_0 exhibits two regimes as a function of $|\langle p \rangle - p_{c0}|$ (see Fig. 12). A nearly perfect network regime occurs when $\langle \Delta R^2 \rangle_0$ is less than $R_0^2/2N^2$, while a disordered network regime appears in the opposite case. In the first case, the resistance noise is directly proportional to the fraction of defects⁴⁹. In the other case (disordered network), the breaking and the recovering of the backbone resistors³⁶ result in an enhancement of the resistance noise. It is noteworthy that the first regime is a finite size effect which disappears in the limit of an infinitely large network⁴⁹. In the second regime the data follow closely the scaling relation:

$$\Sigma_0 \sim |\langle p \rangle - p_{c0}|^{-k} \quad (6)$$

with $k = 3.1$ ⁴⁹. A similar scaling relation, with a different critical exponent $k_f = 1.12$, has been found between the relative variance of resistance fluctuations and $|\langle p \rangle - p_{c0}|$ in the case of 1/f noise in random networks³⁹. On this respect, it must be noticed that the expression 1/f noise is used as a shorthand for a noise (i) spatially uncorrelated, (ii) statistically uniform and (iii) sufficiently small on each elementary resistors of the network to be treated only to the lowest order. Thus, it is this last feature (iii) which makes the crucial difference between the noise in Ref.³⁹ and the Σ_0 noise given by Eq. (6), which instead arises from the random switch-off and switch-on of the elementary resistors. As a consequence, the noise in Eq. (6) is strongly sensitive to the average defect fraction. By combining $\Sigma_0 \sim |\langle p \rangle - p_{c0}|^{-k}$ with $\langle R \rangle_0 \sim |\langle p \rangle - p_{c0}|^{-\mu}$, one obtains in the disordered network regime:

$$\Sigma_0 \sim \langle R \rangle_0^s \quad (7)$$

with $s = k/\mu = 2.6$. A more detailed analysis of the properties of Σ_0 can be found in Ref.⁴⁹.

Now, by considering the behavior of Σ in the nonlinear regime, it is convenient to report its relative variation, $(\Sigma - \Sigma_0)/\Sigma_0$, on a log-log plot as a function on I/I_0 . This is done in Fig. 13, where the same data of Fig. 11 are shown. Similarly to what happens for the average resistance, two regions can be identified in the nonlinear regime. At moderate bias, Σ scales quadratically with the current, as:

$$\frac{\Sigma}{\Sigma_0} = f(I/I_0), \quad f(I/I_0) \simeq 1 + c(I/I_0)^\eta \quad (8)$$

with $\eta = 2.0 \pm 0.1$ and c a dimensionless coefficient. At higher biases, in the pre-breakdown region, a strong superquadratic dependence appears^{50,51}. It must be remarked that the behavior of Σ in the pre-breakdown region is found to be dependent on E_R . In fact, in this region:

$$\frac{\Sigma_I}{\Sigma_0} \sim \left(\frac{I}{I_0}\right)^{\eta_I} \quad (9)$$

with $4.5 \leq \eta_I \leq 5.5$, depending on E_R . Therefore, the straight-line with slope 5 in Fig. 13 has been drawn for a guide to the eyes. This behavior of the relative variance of resistance fluctuations in the pre-breakdown region is different from that obtained in the same region for the average resistance. In fact, as already discussed in connection with Fig. 7, θ_I is found to be practically independent of the E_R value. The strong nonlinearity and nonuniversality of Σ in the pre-breakdown region has been observed in electrical noise measurements in conducting polymers¹⁹ and in other materials^{2,27,45,28}.

The effect on Σ of α and of the different bias conditions (constant current or constant voltage) is considered in Fig. 14. The values of Σ in these figures are obtained from simulations performed for $E_R = 0.043$ (eV) and $r_0 = 1$ (Ω) (as in Figs. 6, 8 and 9). The data indicated by stars and open squares are obtained under constant current conditions with $\alpha = 10^{-3}$ (K^{-1}) and $\alpha = 0$ respectively, while data denoted with triangles and black diamonds are obtained under constant voltage conditions for the two different values of α . Fig. 14 shows that the linear regime value, Σ_0 , is independent of α and bias conditions. By contrast, a significantly different behavior of Σ is found in the nonlinear regime. In particular, the increase of Σ in the pre-breakdown region is steeper under constant current than under constant voltage conditions. This feature is ascribed to the better stability of the RRN under constant voltage, since resistance fluctuations in excess over the mean value are damped in this condition while they are enhanced under constant current conditions. The log-log plots of the relative variation of Σ as a function of I/I_0 and V/V_0 , reported in Figs. 15 and 16 respectively, display the following features. The quadratic dependence of Σ on the bias in the moderate bias region is a feature independent of the values of α and

of the bias conditions. Further investigations, concerning the effect of the network structure and of the geometry of the electrical contacts on this feature are necessary to establish the universality of this behavior. By contrast, the superquadratic behavior in the pre-breakdown region is strongly influenced by both the α value and the bias conditions. Precisely, the simulations in Fig. 15, performed under constant current conditions with $\alpha = 0$ and with $\alpha = 10^{-3}$ (K^{-1}), show a strong enhancement of the relative variance of resistance fluctuations induced at high bias by a positive value of the temperature coefficient of the resistance. On the other hand, by comparing the superquadratic behavior obtained, with $\alpha = 10^{-3}$ (K^{-1}), under constant current conditions and under constant voltage, we can see that the value of η_I is drastically reduced from 5.4 to 3.0 under constant voltage. An extended discussion of these behaviors can be found in Ref.⁵¹.

The Gaussian properties of the fluctuation amplitudes has also been investigated⁵¹. Figure 17 reports the distribution function of the resistance fluctuations $p(R)$ obtained for a bias current $I = 1.8$ (A) (pre-breakdown region). The values of the parameters are the same used for the curves in Fig. 3. The parabola in Fig. 17 represents the fit with a Gaussian distribution. The figure shows a strong enhancement of the probability for the positive fluctuations with respect to the Gaussian distribution. This non-Gaussianity of the fluctuation amplitudes increases at increasing current or at increasing temperature⁵¹, when approaching the breakdown conditions. This emergence of a non-Gaussian behavior near the breakdown can be considered a relevant precursor of failure. Experiments performed in different materials near the electrical breakdown confirm this non-Gaussianity of fluctuations^{29,45,56,57}.

Finally, Fig. 18 displays the spectral densities of resistance fluctuations obtained for two increasing values of the bias current: $I = 1.5$ and $I = 1.8$ (A). The parameters are the same as those in Fig. 17. The spectral densities have been calculated by Fourier transforming the corresponding correlation functions $C_{\delta R}(t)$. The spectra are found to be Lorentzian in agreement with experiments^{4,26,27,45}. Moreover, the analysis of the correlation functions for different bias values and for different substrate temperatures shows that the correlation time is only weakly dependent on the bias while it is strongly dependent on the temperature⁵³.

IV. CONCLUSIONS

I have presented a short review of a recently developed^{50,49,51} approach which allows the study of the resistance noise over the full range of bias values, from the linear regime up to electrical breakdown. Resistance noise is described in terms of two competing processes taking place in RRNs. The two processes consist of the breaking and recovering of the elementary network resistors. The probabilities of the two processes are controlled by an electrical bias and by the external tem-

perature. Monte Carlo simulations are performed to investigate the RRN behavior as a function of the bias; steady state or electrical failure have been found. At the lowest biases, the two processes are practically random and an effective defect generation probability can be defined which controls the network behavior. In this Ohmic regime, a scaling relation has been found between the relative variance of resistance fluctuations and the average resistance⁴⁹. The value of the critical exponent is significantly higher than that associated with 1/f noise. The properties of the nonlinear regime, occurring when the bias overcomes a threshold value, are studied for different values of the material dependent parameters and for different bias conditions (constant voltage or constant current)^{50,51}. In general, two regions can be identified in the nonlinear regime: a moderate bias region, where both the average resistance and the relative variance of resistance fluctuations scale quadratically with the bias, and a pre-breakdown region where these quantities exhibit a superquadratic dependence. The quadratic behavior in the moderate bias region has been found independent of the values of the model parameters and of the bias conditions. A final conclusion about the universality of this behavior requires the investigation of the role of the network topology and of the electrical contact geometry. Remarkably, under constant voltage conditions, it has been found that the average resistance scales quadratically over the full range of voltage values up to breakdown. Moreover, it must be underlined the strong effects on the pre-breakdown properties of the temperature coefficient of the resistance. Furthermore, non-Gaussian noise has been found in the pre-breakdown region under both bias conditions. The results obtained by simulations are found to agree satisfactorily with electrical and noise measurements performed in composites^{2,22,19} and in semicontinuous metal films¹⁶, and in the degradation processes of metallic lines due to electromigration^{26,25}.

ACKNOWLEDGMENTS

I'm grateful to Dr. Z. Gingl and Prof. L. B. Kish who introduced me to the biased percolation approach of failure problems. I also thank Prof. L. Reggiani, Drs. G. Trefan and E. Alfinito who collaborated to these results. Finally I thank INFM for financial support through the STATE project and ASI for support through the project I/R/056/01.

¹ H. J. Herrmann and S. Roux, *Statistical Models for the Fracture of Disordered Media*, North-Holland, Amsterdam (1990).

- ² K. K. Bardhan, B. K. Chakrabarti and A. Hansen, *Nonlinearity and Breakdown in Soft Condensed Matter*, Springer-Verlag, New York (1994).
- ³ A. Bunde and S. Havlin, *Fractals and Disordered Systems*, Springer-Verlag, Berlin (1996).
- ⁴ M. Ohring, *Reliability and Failure of Electronic Materials and Devices*, Academic Press, San Diego (1998).
- ⁵ L. Niemeyer, L. Pietronero and H. J. Wiesmann, *Fractals dimension of dielectric breakdown*, *Phys. Rev. Lett.* **52** (1984) 1033–1036.
- ⁶ L. De Arcangelis, A. Hansen, H. J. Herrmann and S. Roux, *Scaling laws in fracture*, *Phys. Rev. B* **40** (1989) 877–880.
- ⁷ A. Hansen, S. Roux and E. L. Hinrichsen, *Annealed model for breakdown processes*, *Europhys. Lett.* **13** (1990) 517–522.
- ⁸ D. Sornette and C. Vanneste, *Dynamics and memory effects in rupture of thermal fuse networks*, *Phys. Rev. Lett.* **68** (1992) 612–615.
- ⁹ M. Sahimi and S. Arbabi, *Percolation and fracture in disordered solids and granular media: Approach to a fixed point*, *Phys. Rev. Lett.* **68** (1992) 608–611.
- ¹⁰ J. V. Andersen, D. Sornette and K. Leung, *Tricritical behavior in rupture induced by disorder*, *Phys. Rev. Lett.* **78** (1997) 2140–2143.
- ¹¹ S. Zapperi, A. Vespignani and H. E. Stanley, *Plasticity and avalanche behaviour in microfracturing phenomena*, *Nature* **388** (1997) 658–660.
- ¹² S. Zapperi, P. Ray and H. E. Stanley, *First-order transition in the breakdown of disordered media*, *Phys. Rev. Lett.* **78** (1997) 1408–1411.
- ¹³ M. A. Dubson, Y. C. Hui, M. B. Weissman and J. C. Garland, *Measurement of the fourth moment of the current distribution in two-dimensional random resistor networks*, *Phys. Rev. B* **39** (1989) 6807–6815.
- ¹⁴ R. K. Chakrabarti, K. K. Bardhan and A. Basu, *Nonlinear I-V characteristic near the percolation threshold*, *Phys. Rev. B* **44** (1991) 6773–6779.
- ¹⁵ K. K. Bardhan, *Nonlinear conduction in composites above percolation threshold beyond the backbone*, *Physica A* **241** (1991) 267–277.
- ¹⁶ Y. Yagil, G. Deutscher and D. J. Bergman, *Electrical breakdown measurements of semicontinuous metal films*, *Phys. Rev. Lett.* **69** (1992) 1423–1426.
- ¹⁷ M. B. Heaney, *Measurement and interpretation of nonuniversal critical exponents in disordered conductor-insulator composites*, *Phys. Rev. B* **52** (1995) 12477–12480.
- ¹⁸ Z. Rubin, A. Sunshine, M. B. Heaney, I. Bloom and I. Balberg, *Critical behavior of the electrical transport properties in a tunneling-percolating system*, *Phys. Rev. B* **59** (1999) 12196–12199.
- ¹⁹ U. N. Nandi, C. D. Mukherjee and K. K. Bardhan, *1/f noise in nonlinear inhomogeneous systems*, *Phys. Rev. B* **54** (1996) 12903–12914.
- ²⁰ Z. Gingl, C. Pennetta, L. B. Kish and L. Reggiani, *Biased percolation and abrupt failure of electronic devices*, *Semic. Science Techn.* **11** (1996) 1770–1775.
- ²¹ L. Lamainère, F. Carmona and D. Sornette, *Experimental realization of critical thermal fuse rupture*, *Phys. Rev. Lett.* **77** (1996) 2738–2741.
- ²² C. D. Mukherjee, K. K. Bardhan, and M. B. Heaney, *Pre-*

- dictable electrical breakdown in composites, *Phys. Rev. Lett.* **83** (1999) 1215–1218.
- ²³ S. Hirano and A. Kishimoto, *Thermal-electrical breakdown of disordered conductor-insulator composites*, *Jpn. J. Appl. Phys.* **38** (1999) L662–L664.
- ²⁴ C. Pennetta, L. Reggiani and G. Trefan, *Scaling and universality in electrical failure of thin films*, *Phys. Rev. Lett.* **84** (2000) 5006–5009.
- ²⁵ C. Pennetta, L. Reggiani, G. Trefan, F. Fantini, A. Scorzoni and I. De Munari, *A percolative approach to electromigration in metallic lines*, *J. Phys. D: Appl. Phys.* **34** (2001) 1421–1429.
- ²⁶ A. Scorzoni, B. Neri, C. Caprile, and F. Fantini, *Electromigration in thin-film interconnection lines: Models, methods and results*, *Mat. Science Rep.* **7** (1991) 143–220.
- ²⁷ L. K. Vandamme, *Noise as a diagnostic tool for quality and reliability of electronic devices*, *IEEE Trans. on Electron Dev.* **41** (1994) 2176–2187.
- ²⁸ I. Bloom and I. Balberg, *Nonlinear 1/f noise characteristics in luminescent porous silicon*, *Appl. Phys. Lett.* **74** (1999) 1427–1429.
- ²⁹ N. Vandewalle, M. Ausloos, M. Houssa, P. W. Mertens and M. M. Heyns, *Non-Gaussian behavior and anticorrelations in ultrathin gate oxides after soft breakdown*, *Appl. Phys. Lett.* **74** (1999) 1579–1581.
- ³⁰ M. Houssa, T. Nigam, P. W. Mertens and M. M. Heyns, *Soft Breakdown in Ultrathin Gate Oxides: Correlation with the Percolation Theory of Nonlinear Conductors*, *Appl. Phys. Lett.* **73** (1999) 514–516.
- ³¹ G. Trefan, C. Pennetta and L. Reggiani, *A percolative approach to current fluctuations in the soft breakdown of ultrathin oxides*, in *Noise in Physical Systems and 1/f Fluctuations*, Proc. 16th Int. Conf. on Noise in Physical Systems and 1/f Fluctuations, ed. G. Bosman, World Scientific Pub. Co., Singapore (2001) 735–738.
- ³² K. Christensen, R. Donangelo, B. Koiller and K. Sneppen, *Evolution of random networks*, *Phys. Rev. Lett.* **81** (1998) 2380–2383.
- ³³ H. E. Stanley, *Scaling, Universality, and renormalization: Three pillars of modern critical phenomena*, *Rev. Mod. Phys.* **71** (1999) S358–S366.
- ³⁴ R. Albert, H. Jeong and A. L. Barabasi, *Error and attack tolerance of complex networks*, *Nature* **406** (2000) 378 and A. L. Barabasi and R. Albert, *Emergence of scaling in random networks*, *Science* **286** (1999) 509–512.
- ³⁵ A. Gabrielli, G. Caldarelli and L. Pietronero, *Invasion percolation with temperature and the nature of self-organized criticality in real systems*, *Phys. Rev. E* **62** (2000) 7638–7641.
- ³⁶ D. Stauffer and A. Aharony, *Introduction to Percolation Theory*, Taylor & Francis, London (1992).
- ³⁷ M. Sahimi, *Application of Percolation Theory*, Taylor & Francis, London (1994).
- ³⁸ P. M. Duxbury, P. L. Leath and P. D. Beale, *Breakdown properties of quenched random systems: the random fuse networks*, *Phys. Rev. B* **36** (1987) 367–380.
- ³⁹ R. Rammal, C. Tannous, P. Breton and A. M. S. Tremblay, *Flicker (1/f) noise in percolation networks*, *Phys. Rev. Lett.* **54** (1985) 1718 and R. Rammal, C. Tannous and A. M. S. Tremblay, *1/f noise in random resistor networks: fractals and percolating systems*, *Phys. Rev. A* **31** (1985) 2662–2671.
- ⁴⁰ A. A. Snarskii, A. E. Morozovsky, A. Kolek and A. Kusy, *1/f noise in percolation and percolationlike systems*, *Phys. Rev. E* **53** (1996) 5596–5605.
- ⁴¹ K. M. Abkemeier and D. G. Grier, *Topological disorder and conductance fluctuations in thin films*, *Phys. Rev. B* **54** (1996) 2723–2727.
- ⁴² I. Balberg, *Limits on the continuum-percolation transport exponents*, *Phys. Rev. B* **57** (1998) 13351–13354.
- ⁴³ F. N. Hooge, *Experimental studies on 1/f noise*, *Rep. Prog. Phys.* **44** (1981) 479–532 and P. Dutta and P. M. Horn, *Low-frequency fluctuations in solids: 1/f noise*, *Rev. Mod. Phys.* **53** (1981) 497–516.
- ⁴⁴ Y. C. Zhang, *Modelling 1/f noise via dynamical random networks*, *Phys. Rev. B* **36** (1987) 2345–2348.
- ⁴⁵ M. B. Weissman, *1/f noise and other slow, nonexponential kinetics in condensed matter*, *Rev. Mod. Phys.* **60** (1988) 537–571.
- ⁴⁶ B. K. Jones, *The scale invariance of 1/f noise*, in *Unsolved Problems on Noise and Fluctuations*, ed. by D. Abbott and L. B. Kish, A. I. P. (2000) 115–123.
- ⁴⁷ S. T. Bramwell, K. Christensen, J. Y. Fortin, P. C. W. Holdsworth, H. J. Jensen, S. Lise, J. M. Lopez, M. Nicodemi, J. F. Pinton and M Sellitto, *Universal fluctuations in correlated systems*, *Phys. Rev. Lett.* **84** (2000) 3744–3746.
- ⁴⁸ *Noise in Physical Systems and 1/f Fluctuations*, Proc. 16th Int. Conf. on Noise in Physical Systems and 1/f Fluctuations, Gainesville, Florida, ed. by G. Bosman, World Scientific Pub. Co., Singapore (2001).
- ⁴⁹ C. Pennetta, G. Trefan and L. Reggiani, *Scaling law of resistance fluctuations in stationary random resistor networks*, *Phys. Rev. Lett.* **85** (2000) 5238–5241.
- ⁵⁰ C. Pennetta, L. Reggiani, E. Alfinito and G. Trefan, *Stationary regime of random resistor networks under biased percolations*, *Journ. of Phys. C* **14** (2002) 2371–2378.
- ⁵¹ C. Pennetta, L. Reggiani, G. Trefan and E. Alfinito, *Resistance and resistance fluctuations in random resistor networks under biased percolation*, cond-mat/0202268.
- ⁵² L. B. Kish, P. Chaoguang, J. Ederth, W. H. Marlow, C. G. Granqvist and S. S. Savage, *In situ electrical transport measurements and self-organization in gold nanoparticle films during and after deposition*, *Surface and Coating Techn.* **142–144** (2001) 1088–1093.
- ⁵³ C. Pennetta, E. Alfinito and L. Reggiani, unpublished.
- ⁵⁴ C. Pennetta, L. Reggiani and L. B. Kish, *Thermal effects on the electrical degradation of thin film resistors*, *Physica A* **266** (1999) 214–217.
- ⁵⁵ C. Pennetta, L. Reggiani and G. Trefan, *A Monte Carlo percolative approach to reliability analysis of semiconductor structures*, *Mathematics and Comput. in Simulation* **55** (2001) 231–238.
- ⁵⁶ H. T. Hardner, M. B. Weissman, M. Jaime, R. E. Treece, P. C. Dorsey, J. S. Horwitz and D. B. Chrisey, *Non-Gaussian noise in a colossal magnetoresistive film*, *J. Appl. Phys.* **81** (1987) 272–275.
- ⁵⁷ G. T. Seidler, S. A. Solin and A. C. Marley, *Dynamical current redistribution and non-Gaussian 1/f noise*, *Phys. Rev. Lett.* **76** (1996) 3049–3052.